Marine Chemistry
February 2024, Volume 259, Pages 104352 (13p.)
https://doi.org/10.1016/j.marchem.2024.104352 https://archimer.ifremer.fr/doc/00870/98206/

Biogeochemical evidence of flow re-entrainment on the main fringing reef of La Reunion Island

Lagoutte Elsa [1, *], Tribollet Aline [1], Bureau Sophie [2], Cordier Emmanuel [3], Mangion Perrine [2], Chauvin Anne [1], Mouquet Pascal [4], Bigot Lionel [2], Frouin Patrick [2], Cuet Pascale [2]

[1] IRD-Sorbonne Université-CNRS-MNHN, UMR LOCEAN-IPSL, 4 Place Jussieu, Paris Cedex 75005, France
[2] Université de La Réunion-IRD-CNRS-Ifremer-Université de la Nouvelle Calédonie, UMR ENTROPIE - Labex Corail, 15 Avenue René Cassin, CS 92003, Saint-Denis Cedex 9 97744, La Réunion, France
[3] Observatoire des Sciences de l'Univers de La Réunion (OSU-R), UAR3365, Saint-Denis, La Réunion, France
[4] IRD, ESPACE-DEV, Université de La Réunion, Université de Montepellier, Université de Guyane, Université des Antilles, Université de la Nouvelle Calédonie, La Réunion, France

* Corresponding author : Elsa Lagoutte, email address : elsa.lagoutte@ird.fr

Abstract :

Understanding factors influencing seawater chemistry variability in coral reef environments is a major challenge to improve predictions of their evolution in the context of ocean acidification. In this study, autonomous sensors for current speed and direction, photosynthetically active radiation (PAR), temperature, salinity, dissolved oxygen (DO) and pHT were deployed three times between 2021 and 2022 offshore and on three reef flat sites of the main fringing reef of La Reunion Island. Discrete sampling of seawater for DO, pHT and total alkalinity (TA) at different times of the day complemented the monitoring. Diurnal variation of those variables on the reef flat was mainly driven by benthic community metabolism but hydrodynamics and reef geomorphology played also a key role. DO and pHT variations were decoupled in time, especially at night when we observed DO rebounds while pHT values were stationary. The reef flat was also largely TA depleted compared to offshore waters. We hypothesize that the strong offshore-alongshore current redirected TA depleted water exiting from reef channels into the reef flat. This seawater re-entrainment could also explain specific variations of DO and pHT values. This result highlights the important role of reef geomorphology in modulating changes in seawater chemistry. Neglecting this phenomenon could lead to substantial errors in the estimation of carbonate budgets when using the Eulerian approach.

Highlights

► Seawater chemistry on La Saline reef is modulated by hydrodynamics and geomorphology. ► Dissolved oxygen and pH_T variations are decoupled in time on La Saline fringing reef. ► Water exiting the reef by the channels is re-entrained on the reef flat. ► Water re-entrained on the reef flat appears TA depleted. ► The Eulerian approach can lead to errors in the estimation of $CaCO_3$ budgets.

Keywords : Coral reefs, pH sensors, Oxygen sensors, Alkalinity, Carbonate budgets, Hydrodynamics

Introduction

Increasing atmospheric concentrations of anthropogenic carbon dioxide (CO_2) greatly alter the biogeochemical cycles in coastal ecosystems (Orr et al., 2005). The invasion of CO_2 in seawater changes the amount and composition of dissolved inorganic carbon (DIC) species in such a way that the concentration of carbonate ions decreases (Orr et al., 2005), and finally acidifies seawater (Atkinson and Cuet, 2008). Surface ocean pH has already decreased by 0.1 compared to pre-industrial values (Orr et al., 2005) and projection models predict a decline of about 0.04 to 0.29 pH units between the periods 2006-2015 and 2081-2100 depending on the scenario (RCP2.6 or RCP8.5, respectively; Bindoff et al., 2019). This acidification raises many concerns about its effects on marine calcifying organisms and ecosystems such as coral reefs (Hoegh-Guldberg et al., 2007; Guinotte and Fabry, 2008; Schönberg et al., 2017; IPCC, 2019). Several studies showed that ocean warming and ocean acidification (OA) reduce calcium carbonate ($CaCO_3$) production by coral reef benthic organisms (Guinotte and Fabry, 2008; Mollica et al., 2018; Cornwall et al., 2021). Others have shown that OA enhances dissolution of $CaCO_3$ in particular due to changes in the metabolic activity of bioeroding microflora and sponges (Silverman et al., 2009; Andersson and Gledhill, 2013; Schönberg et al., 2017; Tribollet et al., 2009, 2019). Experimental observations suggest that OA could ultimately cause an unbalanced carbonate budget (reef dissolution > accretion; Eyre et al., 2018) but there remains significant uncertainty on projections at the ecosystem scale (Yates and Halley, 2006; Eyre et al., 2018). Some of this uncertainty reflects the use of diverse methodologies and approaches (*ex situ*/ *in situ*), differences in environmental conditions, reef community composition and/or local seawater chemistry but also uncertainties in the estimation of metabolic budgets themselves (Andersson and Gledhill, 2013; Courtney et al., 2016; Courtney and Andersson, 2019).

Coral reefs are exposed to significant fluctuations in seawater chemistry and some studies have shown that they can vary between levels below pre-industrial to future conditions of ocean acidification (Ohde and van Woesik, 1999; Shaw et al., 2012). In shallow coral reef environments, benthic metabolic processes (organic production, respiration, calcification and $CaCO_3$ dissolution; Kinsey, 1985) drive marked daily variations in seawater chemistry. The major biogeochemical processes are net community production (NCP), i.e gross primary production minus respiration, and net community calcification (NCC), i.e $CaCO_3$ precipitation minus dissolution, which depend greatly on the reef community composition (Gattuso et al., 1996). During the day, a positive NCP is generally observed (dominance of phototrophic organisms), increasing dissolved oxygen (DO) and pH while decreasing DIC concentrations. The opposite phenomenon is observed at night due to respiration (NCP<0). A positive NCC decreases total alkalinity (TA) and DIC concentrations in a 2:1 ratio as well as the pH. While a positive NCC usually occurs during the day, net dissolution with NCC<0 can be observed at night (Yates and Halley, 2006). Moreover, changes in reef water chemistry due to these metabolic processes are modulated by local physical parameters such as light intensity stimulating photosynthesis and calcification (Gattuso et al., 1999a; Allemand et al., 2011), hydrodynamic conditions, reef geomorphology and seawater residence time (Falter et al., 2013). Changes in the chemical composition of seawater as it flows over the reef flat are less significant when depth is greater, the width of the reef flat is smaller, seawater residence time is shorter and hydrodynamic conditions are more intense (Falter et al., 2013).

Most *in situ* reef metabolism monitoring methods require measurements of changes in nutrient concentrations and/or carbonate system parameters, associated with some assessment of local hydrodynamics (Barnes, 1983; Kinsey, 1985). The development of autonomous sensors has increased studies with multiple functional scales and with higher temporal resolution worldwide. To date, many studies have focused on a specific point or portion of a reef (e.g. shallow reef; Falter et al., 2008, 2011; barrier reef; Shamberger et al., 2011; Meléndez et al., 2020; back reef; Teneva et al., 2013; atoll; DeCarlo et al., 2017). They have highlighted diel cycles of metabolic processes and provided the possibility for detecting changes due to natural and/or anthropogenic disturbances. Studies on multiple sites within the same reef system (Kekuewa et al., 2021; Pezner et al., 2021; Rintoul et al., 2022) have found that seawater chemistry varies greatly depending on the area considered in the reef, due to changes in benthic community composition and/or physical factors (hydrodynamics, reef geomorphology). Only a few *in situ* studies have conducted measurements on the entire ecosystem at both diel and seasonal scales (high latitude reef; Bates et al., 2010; semi-enclosed reef; Guadayol et al., 2014; shallow reef; Page et al., 2019). These studies provided a pioneer ecosystem-specific framework for predicting future biogeochemical responses to OA. However, local hydrodynamics was not always characterized or clearly explained.

The hydrodynamic forcings driving water circulation through different reef types were described in several studies (Roberts and Suhayda, 1983; Yamano et al., 1998; Lowe et al., 2009; Taebi et al., 2011; Lowe and Falter, 2015). The circulation in coral reefs is mainly induced by incident ocean waves but is also influenced by tides and in some cases wind (Lowe and Falter, 2015).When the waves approach the reef, they break on the reef crest (outer limit of the reef flat and transition with the open ocean) and their breaking causes a rise in the water level; this phenomenon is called set-up (Lowe and Falter, 2015). The pressure gradient due to this set-up then causes a flow through the reef (onshore) towards the back reef and the coast (Lowe et al., 2009). It is balanced by an outflow (offshore) through the passes or small exiting channels (Taebi et al., 2011). Some numerical studies suggested that water exiting through these channels can be re-entrained towards the reef, depending on hydrodynamic forcings and geomorphology of the reef-lagoon-channels system (Herdman et al., 2017; Winter et al., 2020). The modeled re-entrainment could reach 50% of the water exiting (Herdman et al., 2017), suggesting that this process can play an important role on open ocean-lagoon exchanges. Additionally, the development of coupled hydrodynamic-biogeochemical models (Zhang et al., 2011; Zhang et al., 2012; Falter et al., 2013; Dişa et al., 2022) strongly suggested the possible major influence of these forcings on seawater chemistry. For instance, on a section of Ningaloo Reef (Western Australia), Zhang et al. (2011) showed a spatialization of nutrient concentrations (nitrates) and suggested a partial re-entrainment towards the reef flat of nutrient-poor water exiting the channels causing a general drop in nutrient concentration (Zhang et al., 2011).

The purpose of the present study was to evaluate the potential impact of this re-entrainment phenomenon on seawater chemistry and how it could impact metabolic budget calculations. The main fringing reef of La Reunion Island (La Saline) is an ideal location for this as it is a very shallow reef, interrupted by frequent channels, where circulation is driven by waves (Cordier, 2007). This field study made it possible to characterize the natural spatio-temporal variability of seawater chemistry along the fringing reef at La Saline and to identify the influence of the main local factors and physical forcings on this variability.

Materials and methods

Study Sites

Study sites were located on the La Saline fringing reef, western coast of La Reunion Island (Indian Ocean) (Fig. 1). This fringing reef is 9 km long with a width varying between 100 and 600 m (Cordier et al., 2012). It has two major passes (Fig. 1): the 'Ermitage pass' with a width of 80 m and a depth of 5m interrupting the reef and the 'Trois Bassins pass' with a width of 140 m and a depth of 7 m at the southern end of the reef (Cordier et al., 2013). Coral and algal cover at each site was estimated using hyperspectral and multispectral remote sensing data collected in 2015 by Bajjouk et al. (2019). At the site named Trou d'Eau (TDE), located in the southern part of the reef flat close to the Trois Bassins pass, the reef flat (350 m wide) had about 33% coral cover and 56% algal cover. At the site named Livingstone (LIV), located 340 m north of Trou d'Eau, the reef flat (300 m wide) had about 22% coral cover and 65% algal cover. Finally, at the site named Toboggan (TOB), located nearby to the north of the Ermitage pass, the reef flat (250 m wide) had about 21% coral cover and 61% algal cover. Bare sand surface area was 11%, 13% and 18% at TDE, LIV and TOB, respectively. Data were updated with Pléiades satellite images collected in 2021 and 2022. It should be noted that a decrease in coral cover was locally observed, particularly at TOB (Mouquet, unpub).

The La Saline reef is globally characterized by a wave-driven circulation but is also influenced by tide and wind regimes (Cordier, 2007). Significant wave heights (H_s) rarely exceed 2 m, except in winter (Cordier et al., 2012). Past studies highlighted circulation cells on the La Saline fringing reef, influenced by reef geomorphology and hydrodynamic conditions (Cordier et al., 2012). TOB and TDE are preferential areas of oceanic entries flowing towards the back reef; entries which are then divided between a northward and a southward alongshore flow (Cordier et al., 2012). The return of reef water to the ocean takes place through the main Ermitage and Trois Bassins passes or through small channels such as the Planch Alizés channel, north of LIV (Cordier, 2007) (Fig. 1).

Reef surveys

Autonomous measurements of light, temperature, salinity, currents, dissolved oxygen (DO) and pH_T, as well as water discrete sampling, were carried out at TDE in April 2021 (summer) for 15 days, while they were carried out at LIV, TOB and TDE in October 2021 (winter) for 5, 3 and 2 days respectively. In addition, a survey was carried out at TOB in June 2022 (mid-season) for 3 days. Offshore measurements of temperature, salinity and water chemistry were performed at 6-8 m depth 250 m away from the reef crest in April and October 2021, for 14 and 21 days, respectively, but not in June 2022 because of rough hydrodynamic conditions. In addition, previous offshore measurements of currents collected during summer 2019 over 2 months in February-March 2019 as part of the RenovRisk Cyclone project (Bousquet et al., 2021) were included in this study to better characterize offshore hydrodynamic conditions.

Measurements of physical variables

A bottom-mounted acoustic doppler current profiler (AQP for Nortek Aquadopp Profiler) was deployed offshore in February-March 2019 to record 2-min average current speed and direction, every 10 minutes over a vertical profile with cell size of 40 cm. A second bottom-mounted AQP was deployed on the reef flat to record 2-min average current speed and direction, every 5 minutes over a vertical profile with cell size of 10 cm. Both AQPs also recorded instantaneous sea water pressure variations every 10 and 5 minutes offshore and on the reef flat, respectively, in order to monitor tidal fluctuations during the deployment.

Salinity was recorded during sampling offshore using a miniCTD (Valeport) with an accuracy ± 0.01. Salinity and temperature were measured every 15 minutes on the reef flat using a JFE Advantech ACTW-USB probe, with accuracies ± 0.01 and ± 0.1°C, respectively.

Downwelling planar photosynthetically active radiation (PAR) was measured on the reef flat using a Compact LW (Alec-Electronics) recording during 10 seconds every 15 minutes.

DO, pH_T and TA measurements

DO was measured every 15 minutes offshore and on the reef flat using YSI 6920 V2-2 probes equipped with optical O_2 sensors, with an accuracy ± 0.1 $mg.L^{-1}$. The pH_T (total hydrogen ion scale) was measured every 15 minutes using a $SAMI^2$-pH probe (Sunburst Sensors) on the reef flat, with an accuracy ± 0.003 pH units, and a $SeaFET^{TM}$ V2 probe (Sea-bird Scientific) offshore, with an accuracy ± 0.02 pH units.

At each site and sampling period, water samples were collected with a Niskin bottle for DO, pH_T and TA analysis. On two occasions, an automated water sampler (AquaMonitor, GreenEyes) was used to collect TA samples only, at TDE in April 2021 and TOB in June 2022. Samples collected for DO and pH_T analysis were used to check the calibration of the probes. Water samples for analysis of TA were immediately filtered in the field using Whatman GF/F filters. Water samples for pH_T and TA analysis were poisoned with mercuric chloride, following Dickson and Goyet (1994). In total, 31 offshore samples were collected, 15 during the warm season and 16 during the cold one. Reef flat samples were collected at shortest possible time intervals and at different times over the day course. For each sampling period, more than 10 DO and 15 pH_T samples were collected.

DO was measured using the Winkler method according to Aminot and Kérouel (2004). pH_T was measured on the total hydrogen ion scale at 25°C using the potentiometric method described by Dickson and Goyet (1994) and a 905 Titrando Metrohm titrator with a combined pH electrode 6.0253.100. The electrode was calibrated using TRIS (T36) buffers provided by A. Dickson, Scripps Institution of Oceanography. The slope of the electrode was checked each day of measurements with NBS buffers of pH = 4.01, pH = 7.01 and pH = 10.01 (Hanna instruments). pH_T was calculated according the following equation:

$$pH_T = pH_{TRIS} + \frac{E_{TRIS} - E_{sample}}{electrode\ slope}$$

with E the potential difference across the electrode. The precision of the analysis is ± 0.01 pH units (Dickson, 2010). TA was measured in triplicate using an automated potentiometric titration (905 Titrando Metrohm) and calculated from the second inflection point of the titration curve. To approximate the ionic strength of seawater, the acid titrant was 0.01 $mol.L^{-1}$ HCl in NaCl. The HCl concentration was checked each day of measurements using a CRM provided by A. Dickson, Scripps Institution of Oceanography. The precision of the analysis based on triplicate measurements was ± 2 $\mu mol.kg^{-1}$.

Data Processing

Currents

Offshore current speeds were projected on the cross-shore (positive values describe an onshore flow, negative an offshore flow) and alongshore axis (positive values describe an almost northward flow, in direction of the Ermitage pass, negative values in direction of the Trois Bassins pass). On the reef flat the vertical current profiles were depth-averaged according to the definition (Soulsby, 1997) : $U = \frac{1}{h}\int_0^z u(z)dz$ where h is the total water depth and u(z) is the current speed recorded at depth z. In order to identify the main stream flow of water masses over the reef flat, the mean depth-averaged current intensity and direction was computed, and a principal component analysis (Thomson and Emery, 2014) was realized in order to highlight the main and minor axis of variability of the flow. Depth-averaged currents U (m.s^{-1}) were then projected on the axes defined by the mean flow, with the x axis in the direction of the mean flow and the y axis in the direction normal to the mean flow. Angles are reported positively East and negatively West from geographic North.

Carbonate system

Dissolved inorganic carbon (DIC) concentrations, partial pressure of CO_2 (pCO_2) and aragonite saturation state of seawater ($\Omega_{aragonite}$) were estimated with the Matlab program CO_2SYS (van Heuven et al., 2011) using as input data laboratory TA measurements and *in situ* pH_T, temperature and salinity from the probes (the temperature recorded by the SeaFET^{TM} V2 and the JFE Advantech ACTW-USB probe for offshore and reef flat samples, respectively). Typical values of phosphate (0.1 ± 0.02 μmol.kg^{-1}) and silicate concentrations (3 ± 1 μmol.kg^{-1}) were used for open ocean and the reef flat of La Saline fringing reef (Cuet et al., 2011). The constants K_1 and K_2 were from Lueker et al. (2000) as recommended for best practices by Dickson et al. (2007). Propagating uncertainties were estimated using add-ons routines of the Matlab program CO_2SYS (Orr et al., 2018), using probe accuracies (pH, salinity and temperature), precision of the TA analysis, standard deviations around typical values of phosphate and silicate concentrations and default standard errors on dissociation constants and total boron (Orr et al., 2018). For the reef flat, propagating uncertainties on DIC, pCO_2 and $\Omega_{aragonite}$ were 7 μmol.kg^{-1}, 8 μatm and 0.18, respectively. For the open ocean, propagating uncertainties on DIC, pCO_2 and $\Omega_{aragonite}$ were 14 μmol.kg^{-1}, 23 μatm and 0.22, respectively.

TA-DIC relationship

A TA-DIC diagram was used to evaluate the balance between organic carbon metabolism (net community production, NCP) and inorganic carbon metabolism (net community calcification, NCC) according to Suzuki and Kawahata (2003). The relationship between TA and DIC was evaluated by conducting a $TA = m.DIC + b$ regression. The ratio between NCC and NCP was calculated following the equation provided by Suzuki and Kawahata (2003) : $\frac{NCC}{NCP} = \frac{m}{2-m}$ (see also Andersson et al., 2014; Lantz et al., 2014).

Statistics

Data from the probes were smoothed to solve problems of noise filtering (Sharma et al., 2015). The smoothing procedure was carried out with Matlab and was the locally weighted scatterplot smoothing (LOWESS) method (Cleveland, 1979) on a 6-hour window (semidiurnal tide). This method led to the most consistency between raw and smoothed data ($r^2 > 0.97$). Statistical analyses were conducted using R (R Core Team, 2020). Data were first tested for residuals normality and homoscedasticity before comparisons of means (Student's t-test). When these conditions were not respected, nonparametric tests were performed (Mann-Whitney U test). Regressions between TA and DIC were type II Major Axis (MA) using the Smatr package (Warton et al., 2012) because of the symmetric relationship between variables (Bellacicco et al., 2019). Non-significance indicates a p-value > 0.05. Means are indicated ± standard deviation (SD).

Results

Offshore characteristics

Time series of current speeds recorded in 2019 on a vertical profile provided information about offshore boundary currents (Fig. 2). Due to the mixing by swell, the subsurface layer between the surface and 6-8 meter depth was characterized by highly variable cross-shore and alongshore current speeds, without evident pattern. The circulation of the deeper layer was dominated by the alongshore component of the current with current speeds varying between -0.5 and 0.5 m.s^{-1}. They were modulated by the tide with an almost northward current (u >0) at flood tide and a southward current (u<0) at ebb tide (Fig. 2). The cross-shore component of the current was weaker, with current speeds varying between -0.1 and 0.1 m.s^{-1}. They were also modulated by the tide with an onshore current at flood tide and an offshore current at ebb tide.

Offshore temperature, dissolved oxygen (DO) and pH$_T$ were relatively constant over the day. Physical and biogeochemical parameters measured *in situ* were all significantly different between the warm season and the cold one except salinity, with the lowest temperatures and highest DO and pH$_T$ values observed during the cold season (Table 1). DO averages (Table 1) were close to the saturation values estimated from *in situ* temperature and salinity, i.e. 203 ± 1 mmol.m^{-3} during the warm season and 214 ± 2 mmol.m^{-3} the cold one. Offshore total alkalinity (TA) ranged from 2279 to 2294 µmol.kg^{-1} with an average of 2289 ± 4 µmol.kg^{-1} in April 2021 and from 2289 to 2302 µmol.kg^{-1} with an average of 2297 ± 4 µmol.kg^{-1} in October 2021. Offshore concentrations in DIC varied from 1969 to 1988 µmol.kg^{-1} with an average of 1978 ± 5 µmol.kg^{-1} in April 2021 and from 1987 to 2006 µmol.kg^{-1} with an average of 1998 ± 6 µmol.kg^{-1} in October 2021. TA and DIC concentrations varied significantly between the warm and the cold seasons (Table 1). $\Omega_{aragonite}$ varied significantly between the warm and the cold seasons with an average of 3.55 ± 0.06 in April 2021 and an average of 3.36 ± 0.04 in October 2021.

Currents on the reef flat

Current directions and speeds differed greatly among studied sites and/or seasons, although water flow was generally directed onshore over the reef flat (Fig. 3). At TDE during both sets of measurements and TOB in October 2021, the mean current directions were oriented cross-shore with a deviation from the cross-shore axis of less than 10°. At LIV in October 2021 and TOB in June 2022, deviations from the cross-shore axis were 57° and 44° north, respectively. At LIV and TDE in October 2021, the mean current flow was weaker than its variability due to frequent reversals reducing the net water flux. Over the 15 days of measurements at TDE in April 2021, reversals of current also occurred but the mean current flow over the period was stronger than its variability. At TOB, the principal components of the current were not clear with an ellipse which is more round than ellipsoidal, certainly due to the large range of current directions with high current speed in most directions.

Diel variations of DO, pH$_T$, temperature and PAR on the reef flat

On the reef flat, diel variations of DO concentration, pH$_T$ and temperature largely exceeded offshore variability due to reef benthic metabolism and low depth on the reef flat (Fig. 3). General trends did not vary among studied sites or periods. Similarly, salinity was relatively homogeneous in space and time (Table 2). The highest DO values occurred at midday when PAR values were the highest. The lowest DO values occurred at night, sometimes just at the beginning of the night (Fig. 3). These variations are in good agreement with metabolic processes (O$_2$ release by day, when photosynthesis exceeds respiration and nighttime uptake by respiration). The highest pH$_T$ values and temperatures occurred in the afternoon (~3:00 pm), out of step with PAR and DO, while the pH$_T$ minimum occurred at the end of the night (~6:00 am).

The greatest diel range of DO, pH$_T$ and temperature was observed at LIV in October 2021 (Fig. 3, Table 3), certainly due to the lowest mean current speed (Table 4). The lowest diel ranges were observed at TOB, which had the highest mean current speed and the shortest reef flat width.

Short monitorings of DO and pH$_T$ (a few days) showed high variability from one day to another, mostly around maxima and minima (Fig. 3). The best example was TDE in October 2021 with 2 days of measurements completely different (Supplementary Material S1.3). In contrast, the acquisition of data over a long period of time (15 days) at TDE in April 2021 provided smooth daily average curves even though hydrodynamic conditions and PAR varied greatly over time.

To illustrate variability from one day to the next, time series from the longest monitoring (15 days) at TDE in April 2021 are reported on Figure 4. The total water depth variations on the reef flat, including tidal variations and set-up induced by incoming waves, ranged between 0.9 and 1.7 m. The highest diel ranges of DO and pH$_T$ were 200 mmol.m^{-3} and 0.34 respectively and occurred on 4 days (from 29 April to 02 May) during fair hydrodynamic conditions (current speed < 0.1 m.s^{-1} and water depth < 1 m), between a spring and a neap tide. The lowest diel ranges of DO and pH$_T$ were 78 mmol.m^{-3} and 0.15 respectively, when water depth was ~1.5 m and current speed ~ 0.3 m.s^{-1}, and occurred during 3 consecutive days (03-05 May), during neap tide and a swell event.

Rebounds in DO concentration and stationary phases of pH$_T$ values were observed at night during the rising tide demonstrating an influx of waters with higher DO and pH$_T$, mainly occurring on days with highest tides (Fig. 4 and Supplementary Material S1). Conversely, when the tidal range was low, DO remained relatively constant and pH$_T$ decreased progressively overnight. Such rebounds were also observed in temperature time series at LIV in October 2021 and at TDE in October 2021 (Supplementary Material S1) suggesting an influx of warmer water than reef flat waters. Those phenomena were not apparent by day during the rising tide.

Carbonate system parameters on the reef flat

Seawater carbonate chemistry was highly variable on the reef flat over diel timescale (Fig. 5). TA varied daily with maximum values during the night, but never reached offshore values (Fig. 5). No seasonal trend was detected, either at the site or reef flat scale (La Saline). Variability between consecutive days of measurements at a single site was of the same magnitude as the variability among sites, especially during the day. During the night, TA and DIC concentrations were more homogeneous, mainly from midnight to sunrise.

$\Omega_{aragonite}$ ranged between 2.43 and 4.49 depending on the time of the day (Fig. 6). Minimum values ($\Omega_{aragonite}$ < offshore $\Omega_{aragonite}$) occurred at night, when DIC concentrations were higher on the reef flat than offshore. The slopes of the three TA-DIC regressions (type II, MA) calculated for TDE (April 2021 and October 2021) and TOB (June 2022) were not significantly different (*p*-value = 0.56). Regressions for LIV and TOB in October 2021 were not performed because of the low number of samples. For the entire data set, TA was related to DIC by the equation : TA = 0.394xDIC + 1475 (r^2 = 0.87, *p*-value < 0.001) with a 95% confidence interval around the slope of [0.363 ; 0.425]. A 0.394 (± 0.03) slope corresponded to a NCC that was 24 (± 2) % of NCP.

Mean offshore TA values did not fall on the line of the linear regression (Fig. 6). Only three points from Toboggan in October 2021 (stars) were close to offshore TA and DIC values. Those samples corresponded to a period of strong hydrodynamic conditions (Supplementary Material S1.2).

Discussion

Biogeochemistry variability on La Saline fringing reef

Higher DO concentration generally occurred near midday while higher temperatures and pH$_T$ as well as lower TA and DIC were observed between midday and sunset, at around 3:00 pm, except at TOB in June 2022 (Fig. 3, Fig. 4 and Fig. 5). Lowest DO concentrations always occurred at night while lowest pH$_T$ and temperatures occurred at the end of the night. Such diel pattern in seawater carbonate chemistry (pH$_T$, DIC, TA) has been commonly observed worldwide (Hofmann et al., 2011; Albright et al., 2013; Cyronak et al., 2020) but this is the first time that lags between local extremes of DO and carbonates parameters on a reef flat are reported. Several authors (Gray et al., 2012; Koweek et al., 2015b; De Carlo et al., 2017; Bolden et al., 2019; Page et al., 2019; Kekuewa et al., 2021; Pezner et al., 2021; Rintoul et al., 2022) observed indeed a good concordance between DO and carbonate parameters on various types of reef flats and/or lagoon. In the present study, efforts were made to check the calibration of the DO and pH$_T$ probes using several discrete water samples. Probes and sample values were in good agreement ($r^2 \geqslant 0.98$) indicating that there was no methodological nor analysis bias. This suggests that time lags in local minima and maxima between DO and pH$_T$ resulted from a natural process on the fringing reef at La Reunion Island. While DO concentration is only affected by photosynthesis and respiration, calcification reduces pH, partly compensating for increases in pH due to photosynthesis during the day. Rintoul et al. (2022) suggested this might be responsible for the observed decoupling of DO and pH$_T$ in the channel of the Okinawa fringing reef, Japan (decoupling not observed on the reef flat or lagoon). Hysteresis in diurnal cycles of net photosynthesis and calcification was previously reported both in corals (Levy et al., 2004; Schneider et al., 2009) and on coral reef flats (Shaw et al., 2015). On coral reef flats, higher net calcification to net photosynthesis ratios were observed in the afternoon, either because photosynthesis is usually reduced in the afternoon compared to the morning (see Levy et al., 2004), or because the aragonite saturation state is higher in the afternoon relative to the morning for any given net photosynthesis value, favoring calcification (Shaw et al., 2015). This should however result in higher pH$_T$ values in the morning relative to the afternoon, which is not the case at La Saline reef. In contrast, higher net photosynthetic rates were observed in the afternoon compared to the morning when different coral species were exposed to the same PAR values (Levy et al., 2004; Schneider et al., 2009), presumably due to higher respiration rates of the host tissue in the morning. In this case, Schneider et al. (2009) found that ΔpH (pH final – pH initial) was negative for an additional 2–3 h after oxygen concentration began to rise (about 3 h after sunrise), indicating a pH decrease induced by a higher net calcification rate than net photosynthesis. Similarly, the slow increase in pH_T recorded in the morning on La Saline reef compared to DO suggests that photosynthetic activity on the reef flat may not compensate for the decrease in pH_T due to calcification until several hours after sunrise. Community respiration is high on La Saline reef, due to anthropogenic nutrient inputs (Tedetti et al., 2020) leading to elevated organic production (Cuet et al., 2011). By the end of the night, seawater is severely depleted in oxygen and pH_T is remarkably low downstream of the reef flat. The factor explaining why calcification outweighs photosynthetic activity in the early hours of the day could therefore be an influx of seawater from the back-reef zone towards the reef flat, favored by the frequently observed outflow currents (Fig. 3). Mixing with oceanic water passing through the reef could limit the photosynthesis-related increase in pH_T, making the impact of calcification on pH_T particularly significant.

In addition to these biological processes, physical processes are likely to be involved. In shallow reef environments, diffusion between seawater and atmosphere can occur (Falter et al., 2008), especially when low tide coincides with the maximum metabolic activity of the benthic community (Gruber et al., 2017). The La Saline fringing reef can be exposed to extreme DO over- and under-saturation due to low depth and high productivity of the reef (Cuet et al., 2011). It results in a loss to the atmosphere or an entry in seawater of oxygen, during the day and at night respectively. We can thus hypothesize that a more rapid exchange of O_2 with the atmosphere, compared to CO_2, contributes to the observed time lags between extremes of DO and pH_T in the specific case of La Saline fringing reef. CO_2 diffusion into the atmosphere is generally considered negligible during the few hours that water is transiting over fringing reefs (Koweek et al., 2015b; Bolden et al., 2019), thus marginally affecting the pH_T of seawater.

Influence of hydrodynamic conditions

The observed amplitude of mean diel variations on the La Saline fringing reef was similar to that reported in other shallow wave-driven reef systems such as Kaneohe Bay reefs (Hawaii; Falter et al., 2008). At La Saline, part of the large observed diel variations was due to the reef communities' metabolism, because of nutrient originating from landbased human activities (Tedetti et al., 2020) leading to elevated organic production and respiration rates (Cuet et al., 2011). DO and pH_T variations were also strongly influenced by the hydrodynamic conditions depending on the day data were collected (Fig. 4; see also Supplementary Material S1). The lowest amplitudes were associated with increases in water depth and current speeds, consistent with previous observations. At Kaneohe Bay, DO daily variations were found to vary between 40 $mmol.m^{-3}$ and 150 $mmol.m^{-3}$ depending on offshore significant wave height (Falter et al., 2008). At Heron reef (Australia), Kekuewa et al. (2021) showed that the biogeochemical signal resulting from the reef communities' metabolism was greatly diluted at 2.22 m depth compared to 0.63 m depth (average diel range of DO, 59 ± 17 $\mu mol.kg^{-1}$ and 137 ± 45 $\mu mol.kg^{-1}$ respectively). In this study, the variability in the amplitudes of DO and pH_T variations was greatest during the shortest measurements due to different hydrodynamics conditions (Fig. 3; see also Supplementary Material S1). On the contrary, Koweek et al. (2015b) showed that stable hydrodynamic conditions during 6 days on the fringing reef of Ofu Island (American Samoa) led to relatively constant amplitudes of DO and pH variations. These results suggest that the interpretation of short surveys may be biased, and point to the need for measurements over at least 1-2 weeks to capture the natural variability of reef seawater chemistry.

In the present study, rebounds in DO and temperature were observed at night during the rising tide while pH_T remained constant (Fig. 4; see also Supplementary Material S1). This behavior is presumably due to incoming offshore water with higher temperature, oxygen and pH_T (Fig. 3). Such anomalies were not observed by day because they were hidden by the strong variations linked to the benthic metabolic activity. Falter et al. (2013) suggested that this phenomenon could result from a re-entrainment into the cross-reef flow of water which exited the reef through channels. Their model showed diurnal variations in pCO_2 (counterpart of O_2) on their hypothetical reef flat with truncated nighttime maxima (Falter et al., 2013). A re-entrainment of low pCO_2 water produced during the day could thus mitigate maximum nighttime values (Falter et al., 2013). Similarly, Koweek et al. (2015b) observed truncated nighttime minima on their time series of temperature, DO and pH_T while in the case of Rintoul et al. (2022)'s study, only nighttime minima temperature and pH_T were truncated.

Total alkalinity anomaly: an evidence of flow re-entrainment

Changes in TA were quantitatively smaller than changes in DO, pH_T and DIC, probably due to the higher importance of photosynthesis and respiration processes compared to calcification and $CaCO_3$ dissolution (Pezner et al., 2021). Theoretically, DIC concentrations and TA are lower on a reef flat than offshore during the day due to the photosynthesis (DIC uptake) and $CaCO_3$ precipitation (DIC uptake and TA decrease) by calcifying organisms such as corals and crustose coralline algae when they are healthy and abundant (Suzuki and Kawahata, 2003; Watanabe et al., 2006; Lantz et al., 2014; DeCarlo et al., 2017; Cyronak et al., 2018). The opposite trend is observed at night when respiration and $CaCO_3$ dissolution occur and induce high DIC concentrations and TA. In our study, we systematically measured a much higher TA offshore compared to the reef flat, even at night when DIC was lower offshore (Fig. 5, Fig. 6). Our offshore TA measurements were consistent with a prior study conducted nearby by Chauvin (2013). Our values were also similar to those reported on reef slopes of other Indo-Pacific reefs (Watanabe et al., 2006; Lantz et al., 2014; Koweek et al., 2015a; Page et al., 2019) and in agreement with the typical value for worldwide tropical surface waters (2300 $\mu mol.kg^{-1}$, Lee et al., 2006). This suggests that there was no sampling nor analysis bias with our offshore samples. Page et al. (2019) observed a similar offset between the Kaneohe Bay reef flat and the oceanic station ALOHA that they attributed to a high rate of calcification on the reef flat. It is common however to observe that the points on the TA-DIC diagram fall along a line radiating to the left or right from a point that represents the mean TA and DIC properties of the ocean source water (see Muehllehner et al., 2016). Based on TA values and other measured parameters, we calculated that net calcification (G_{net}) was about 40% of gross community production (P) at Trou d'Eau in October 2021 (not shown in this study; see Supplementary Material S2 for the detailed calculations using an Eulerian method of flow respirometry with the DO measurements for P). Daily net calcification is usually about 15-20 % of gross community production (Gattuso et al., 1999a; Falter et al., 2013). While P at Trou d'Eau in October 2021 (726 $mmolC.m^{-2}.d^{-1}$) was similar to the Indo-Pacific median given by Falter et al. (2013) (reevaluation of the Kinsey's standard rates; Kinsey 1985), G_{net} (283 $mmolC.m^{-2}.d^{-1}$) was much higher. This result is particularly surprising given the relatively low coral cover of La Saline fringing reef (33% at Trou d'Eau). A G_{net} rate similar to the one calculated at La Reunion Island was found at Yonge Reef (Great Barrier Reef, Australia) but with a coral cover up to 60 % (Gattuso et al., 1996). Moreover, Cuet et al. (2011) previously measured a much lower G_{net} / P ratio (21%) at Trou d'Eau using a Lagrangian approach. Assessment of ecosystem functions can also be performed using plots of TA as a function of DIC (Andersson et al., 2014; Lantz et al., 2014). In the present study, the relationships between TA and DIC concentrations were not significantly different across sites and seasons, suggesting similar benthic community structure (Takeshita et al., 2018). The NCC represented 24% of the NCP, a common ratio for Indo-Pacific reefs and in good agreement with ratios worldwide between 14% and 52% (Cyronak et al., 2018). Thus, we hypothesize that water flowing over the reef crest was TA depleted compared to the offshore water. The offset in our TA-DIC diagram is most probably explained by the re-entrainment of a part of the water that freshly exited the reef flat through the passes or channels and that was depleted in TA due to the daylight activity of the benthic community. This is in agreement with the results of the Falter et al. (2013)'s model and suggests that rebounds in DO concentration observed at night were not only due to oceanic inputs during the rising tide. However, it is likely that DO concentration is much less affected by this phenomenon because of the exchanges between seawater and atmosphere during the re-circulation and the breaking of the waves (Frankignoulle et al., 1996). The breaking of the waves on the reef crest could indeed favor the chemical equilibrium of oxygen with the atmosphere leading to a potential good concordance between DO concentration offshore and in waters flowing over the reef crest.

Implications for using the Eulerian method to estimate metabolic budgets

Net reef ecosystem metabolic rates are often estimated from changes in water chemistry relative to some reference point (usually offshore) taking into account the residence time of seawater in the area (Gattuso et al., 1997; Bates et al., 2010; Shamberger et al., 2011; Albright et al., 2013; Lantz et al., 2014; DeCarlo et al., 2017; McMahon et al., 2018; Bolden et al., 2019; Pezner et al., 2021). It is generally assumed that water exiting a reef system is mainly replaced by water from the open ocean (Winter et al., 2020). When reefs are intercepted by channels, such as the fringing reef of La Reunion Island, it seems irrelevant to consider those systems as simple boxes with exchanges between homogenous oceanic water and the reef water only (Zhang et al., 2012). It could lead to miscalculation of metabolic budgets due to the re-entrainment of TA depleted water into the reef flat. Courtney and Andersson (2019) and Courtney et al. (2021) suggested that the main uncertainty in the estimation of net reef calcification is due to uncertainties about hydrodynamics. In a simple box-type model, they simulated the effects of uncertainty in water depth and residence time on net ecosystem calcification (NEC). They showed that an 83% underestimation of the residence time can lead to an overestimation of the NEC by 500% while an 83% overestimation of the residence time can lead to underestimate the NEC by 45%. Neglecting the re-entrainment effect on the estimation of the residence time could therefore lead to important errors in NEC assessment. In the present study, this phenomenon greatly affected our calculations and therefore introduced a substantial error in the estimation of the carbonate budget that the Lagrangian method used by Cuet et al. (2011) makes it possible to avoid.

Falter et al. (2013) suggested that the re-entrainment effect influences water chemistry at a local scale only (few hundreds of meters). This result was based on an idealized reef geomorphology and constant offshore forcings (stationary offshore wave forcing, constant southward offshore currents). Because of the many differences between the hypothetical reef of Falter et al. (2013) and La Saline reef, it is difficult to assess the possible spatial extent of the influence of re-entrainment on seawater chemistry for the present case study. Winter et al. (2020) modelized flow re-entrainement in wave-dominated coastal reef systems, as well as the impact of different oceanic forcings and reef geometry. They showed that the magnitude of the water current running along the reef is an important oceanic forcing of the flow re-entrainment. In their model, a strong offshore alongshore current (> 0.15 $m.s^{-1}$), similar to the one observed along the fringing reef of La Reunion Island (Fig. 2), increases the re-entrainment phenomena whatever the reef geometry and the hydrodynamic conditions. They also showed that reefs with many channels and an exposure to large waves have higher re-entrainment rates. The effect of the re-entrainment was observed at all our studied sites, yet at different distances from the passes and channels. Surprisingly, TA depleted water did not reach the offshore site located 250 meters from the reef crest, therefore probably too far from the area of water mixing (Fig. 1). The fact that the metabolic rates of reef ecosystems obtained with the Eulerian approach are highly dependent on hydrodynamics highlights the crucial need to better understand coastal circulation prior to metabolic studies.

Conclusions

The present study showed that variability of seawater parameters on the La Saline reef flat is strongly controlled by benthic metabolic activity and by water depth, geomorphology, hydrodynamic forcing and residence time. Compared to other recent *in situ* coral reef studies (Koweek et al., 2015b; Page et al., 2019; Kekuewa et al., 2021; Pezner et al., 2021; Rintoul et al., 2022), our results showed for the first time at a reef and ecosystem scale, the importance of the process of offshore water re-entrainment on seawater parameters and the estimation of the carbonate budget on the La Saline reef flat. The strong offset between offshore total alkalinity and reef flat total alkalinity was mainly the result of flow re-entrainment due to reef geomorphology and strong alongshore current outside the reef (Winter et al., 2020; Dişa et al., 2022) but not to a high rate of net calcification. As net calcification was previously shown to respond positively to alkalinity increase (Albright et al., 2016), the potential effect of TA depleted re-entrained waters on calcification rates remains to be evaluated. Due to this phenomenon, measuring changes in water chemistry on the reef flat with reference to offshore conditions did not allow assessing a relevant carbonate budget. Measurements near the reef crest instead of offshore (i.e. 250 m away from the reef crest) might help resolving the issue. However, as in most wave-exposed fringing reef systems, the reef crest is not easily accessible for measurements due to wave breaking. We conclude that coupled hydrodynamic-biogeochemical models should be improved by quantifying the impact of re-entrainment on reef flat seawater chemistry in shallow coral reefs, depending on specific characteristics of the studied systems.

Data availability

The data that supports the finding of this study are available at https://doi.org/10.26171/KHYE-3813.

Samples CRediT author statement

Elsa Lagoutte: Methodology, Software, Formal Analysis, Investigation, Data Curation, Writing - Original Draft, Visualization. **Aline Tribollet:** Investigation, Resources, Writing - Original Draft, Supervision, Project administration, Funding acquisition. **Sophie Bureau:** Investigation, Data Curation, Writing - Review & Editing. **Emmanuel Cordier:** Software, Validation, Resources, Data Curation, Supervision, Writing - Review & Editing. **Perrine Mangion:** Investigation, Data Curation, Writing - Review & Editing. **Anne Chauvin:** Investigation, Data Curation, Writing - Review & Editing. **Pascal Mouquet:** Formal Analysis, Writing - Review & Editing. **Lionel Bigot:** Investigation, Writing - Review & Editing. **Patrick Frouin:** Investigation, Writing - Review & Editing. **Pascale Cuet:** Conceptualization, Methodology, Validation, Investigation, Resources, Writing - Original Draft, Supervision, Project administration, Funding acquisition.

Acknowledgments

The authors would like to thank the Observatoire des Sciences de l'Univers de La Réunion (OSU-Réunion) for the support provided for this study. We would like to thank, in particular, Jean-Pierre Cammas (OSU-R director) for the coordination of the RenovRisk Transfert project and the technical team of OSU-R (Sophie Ferreira, Pierre Stamenoff and Yoan Benoit). We also would like to thank Claude Mignon from the laboratory LOCEAN for his help during one field work. Access to Pleiades satellite images was granted by the CNES programs Dinamis and Kalideos Réunion.

Funding

This work was supported by the Fonds européen de développement régional (FEDER) for the RenovRisk Transfert project, by a Belmont Forum International for the International and interdisciplinary project 'Evaluation, Mitigation and Adaptation of impacts of Ocean Acidification to Marine Ecosystem' (OA-ME) and by an Office français de la Biodiversité (OFB) France Relance - EU Next Generation project Future Maore Reefs project.

Appendix A. Supplementary data

References

Albright, R., Caldeira, L., Hosfelt, J., Kwiatkowski, L., Maclaren, J.K., Mason, B.M., Nebuchina, Y., Ninokawa, A., Pongratz, J., Ricke, K.L., Rivlin, T., Schneider, K., Sesboüé, M., Shamberger, K., Silverman, J., Wolfe, K., Zhu, K., Caldeira, K., 2016. Reversal of ocean acidification enhances net coral reef calcification. Nature 531, 362–365. https://doi.org/10.1038/nature17155

Albright, R., Langdon, C., Anthony, K.R.N., 2013. Dynamics of seawater carbonate chemistry, production, and calcification of a coral reef flat, central Great Barrier Reef. Biogeosciences 10, 6747–6758. https://doi.org/10.5194/bg-10-6747-2013

Allemand, D., Tambutté, E., Zoccola, D., Tambutté, S., 2011. Coral calcification, Cells to reef, in: Dubinsky, Z., Stambler, N. (Eds.), Coral Reefs: An Ecosystem in Transition. Springer Dordrecht, pp. 119–150. https://doi.org/10.1007/978-94-007-0114-4_9

Aminot, A., Kérouel, R., 2004. Hydrologie des écosystèmes marins: paramètres et analyses, Ed. Ifremer.

Andersson, A.J., Gledhill, D., 2013. Ocean Acidification and Coral Reefs: Effects on Breakdown, Dissolution, and Net Ecosystem Calcification. Annu. Rev. Mar. Sci. 5, 321–348. https://doi.org/10.1146/annurev-marine-121211-172241

Andersson, A.J., Yeakel, K.L., Bates, N.R., de Putron, S.J., 2014. Partial offsets in ocean acidification from changing coral reef biogeochemistry. Nature Clim Change 4, 56–61. https://doi.org/10.1038/nclimate2050

Atkinson, M., Cuet, P., 2008. Possible effects of ocean acidification on coral reef biogeochemistry: topics for research. Mar. Ecol. Prog. Ser. 373, 249–256. https://doi.org/10.3354/meps07867

Bajjouk, T., Mouquet, P., Ropert, M., Quod, J.-P., Hoarau, L., Bigot, L., Le Dantec, N., Delacourt, C., Populus, J., 2019. Detection of changes in shallow coral reefs status: Towards a spatial approach using hyperspectral and multispectral data. Ecological Indicators 96, 174–191. https://doi.org/10.1016/j.ecolind.2018.08.052

Barnes, D.J., 1983. Profiling coral reef productivity and calcification using pH and oxygen electrodes. Journal of Experimental Marine Biology and Ecology 66, 149–161. https://doi.org/10.1016/0022-0981(83)90036-9

Bates, N.R., Amat, A., Andersson, A.J., 2010. Feedbacks and responses of coral calcification on the Bermuda reef system to seasonal changes in biological processes and ocean acidification. Biogeosciences 7, 2509–2530. https://doi.org/10.5194/bg-7-2509-2010

Bellacicco, M., Vellucci, V., Scardi, M., Barbieux, M., Marullo, S., D’Ortenzio, F., 2019. Quantifying the Impact of Linear Regression Model in Deriving Bio-Optical Relationships: The Implications on Ocean Carbon Estimations. Sensors 19, 3032. https://doi.org/10.3390/s19133032

Bindoff, N.L., Cheung, W.W.L., Kairo, J.G., Arístegui, J., Guinder, V.A., Hallberg, R., Hilmi, N., Jiao, N., Karim, M.S., Levin, L., O’Donoghue, S., Purca Cuicapusa, S.R., Rinkevich, B., Suga, T., Tagliabue, A., Williamson, P., 2019. Changing Ocean, Marine Ecosystems, and Dependent Communities, in: Pörtner, H.-O., Roberts, D.C., Masson-Delmotte, V., Zhai, P., Tignor, M., Poloczanska, E., Mintenbeck, K., Alegría, A., Nicolai, M., Okem, A., Petzold, J., Rama, B., Weyer, N.M. (Eds), IPCC Special Report on the Ocean and Cryosphere in a Changing Climate. Cambridge University Press, Cambridge, UK and New York, NY, USA, pp. 447-587. https://doi.org/10.1017/9781009157964.007

Bolden, I.W., Sachs, J.P., Gagnon, A.C., 2019. Temporally-variable productivity quotients on a coral atoll: Implications for estimates of reef metabolism. Marine Chemistry 217, 103707. https://doi.org/10.1016/j.marchem.2019.103707

Bousquet, O., Barruol, G., Cordier, E., Barthe, C., Bielli, S., Calmer, R., Rindraharisaona, E., Roberts, G., Tulet, P., Amelie, V., Fleischer-Dogley, F., Mavume, A., Zucule, J., Zakariasy, L., Razafindradina, B., Bonnardot, F., Singh, M., Lees, E., Durand, J., Mekies, D., Claeys, M., Pianezze, J., Thompson, C., Tsai, C.-L., Husson, R., Mouche, A., Ciccione, S., Cattiaux, J., Chauvin, F., Marquestaut, N., 2021. Impact of Tropical Cyclones on Inhabited Areas of the SWIO Basin at Present and Future Horizons. Part 1: Overview and Observing Component of the Research Project RENOVRISK-CYCLONE. Atmosphere 12, 544. https://doi.org/10.3390/atmos12050544

Chauvin, A., 2013. Photosynthèse et calcification sur les récifs coralliens face au changement global et aux impacts anthropiques : du corail hermatypique *Acropora Muricata* à l’écosystème. Université La Réunion.

Cleveland, W.S., 1979. Robust Locally Weighted Regression and Smoothing Scatterplots. Journal of the American Statistical Association 74, 829–836.

Cordier, E., 2007. Dynamique hydrosédimentaire du récif frangeant de l’Hermitage / La Saline (La Réunion): processus physiques et flux sédimentaires (Océanographie physique- Sédimentologie). Université La Réunion.

Cordier, E., Lézé, J., Join, J.-L., 2013. Natural tidal processes modified by the existence of fringing reef on La Reunion Island (Western Indian Ocean): Impact on the relative sea level variations. Continental Shelf Research 55, 119–128. https://doi.org/10.1016/j.csr.2013.01.016

Cordier, E., Poizot, E., Méar, Y., 2012. Swell impact on reef sedimentary processes: A case study of the La Reunion fringing reef. Sedimentology 59, 2004–2023. https://doi.org/10.1111/j.1365-3091.2012.01332.x

Cornwall, C.E., Comeau, S., Kornder, N.A., Perry, C.T., van Hooidonk, R., DeCarlo, T.M., Pratchett, M.S., Anderson, K.D., Browne, N., Carpenter, R., Diaz-Pulido, G., D’Olivo, J.P., Doo, S.S., Figueiredo, J., Fortunato, S.A.V., Kennedy, E., Lantz, C.A., McCulloch, M.T., González-Rivero, M., Schoepf, V., Smithers, S.G., Lowe, R.J., 2021. Global declines in coral reef calcium carbonate production under ocean acidification and warming. Proc. Natl. Acad. Sci. U.S.A. 118, e2015265118. https://doi.org/10.1073/pnas.2015265118

Courtney, T.A., Andersson, A.J., 2019. Evaluating measurements of coral reef net ecosystem calcification rates. Coral Reefs 38, 997–1006. https://doi.org/10.1007/s00338-019-01828-2

Courtney, T.A., Andersson, A.J., Bates, N.R., Collins, A., Cyronak, T., de Putron, S.J., Eyre, B.D., Garley, R., Hochberg, E.J., Johnson, R., Musielewicz, S., Noyes, T.J., Sabine, C.L., Sutton, A.J., Toncin, J., Tribollet, A., 2016. Comparing Chemistry and Census-Based Estimates of Net Ecosystem Calcification on a Rim Reef in Bermuda. Front. Mar. Sci. 3. https://doi.org/10.3389/fmars.2016.00181

Courtney, T.A., Cyronak, T., Griffin, A.J., Andersson, A.J., 2021. Implications of salinity normalization of seawater total alkalinity in coral reef metabolism studies. PLoS ONE 16, e0261210. https://doi.org/10.1371/journal.pone.0261210

Cuet, P., Atkinson, M.J., Blanchot, J., Casareto, B.E., Cordier, E., Falter, J., Frouin, P., Fujimura, H., Pierret, C., Susuki, Y., Tourrand, C., 2011. CNP budgets of a coral-dominated fringing reef at La Réunion, France: coupling of oceanic phosphate and groundwater nitrate. Coral Reefs 30, 45–55. https://doi.org/10.1007/s00338-011-0744-4

Cyronak, T., Andersson, A.J., Langdon, C., Albright, R., Bates, N.R., Caldeira, K., Carlton, R., Corredor, J.E., Dunbar, R.B., Enochs, I., Erez, J., Eyre, B.D., Gattuso, J.-P., Gledhill, D., Kayanne, H., Kline, D.I., Koweek, D.A., Lantz, C., Lazar, B., Manzello, D., McMahon, A., Meléndez, M., Page, H.N., Santos, I.R., Schulz, K.G., Shaw, E., Silverman, J., Suzuki, A., Teneva, L., Watanabe, A., Yamamoto, S., 2018. Taking the metabolic pulse of the world’s coral reefs. PLoS ONE 13, e0190872. https://doi.org/10.1371/journal.pone.0190872

Cyronak, T., Takeshita, Y., Courtney, T.A., DeCarlo, E.H., Eyre, B.D., Kline, D.I., Martz, T., Page, H., Price, N.N., Smith, J., Stoltenberg, L., Tresguerres, M., Andersson, A.J., 2020. Diel temperature and pH variability scale with depth across diverse coral reef habitats. Limnol Oceanogr Letters 5, 193–203. https://doi.org/10.1002/lol2.10129

DeCarlo, T.M., Cohen, A.L., Wong, G.T.F., Shiah, F., Lentz, S.J., Davis, K.A., Shamberger, K.E.F., Lohmann, P., 2017. Community production modulates coral reef pH and the sensitivity of ecosystem calcification to ocean acidification. J. Geophys. Res. Oceans 122, 745–761. https://doi.org/10.1002/2016JC012326

Dickson, A.G., 2010. The carbon dioxide system in seawater: equilibrium chemistry and measurements, in: Riebesell, U., Fabry, V.J., Hansson, L., Gattuso, J-P. (Eds), Guide to Best Practices for Ocean Acidification Research and Data Reporting. Luxembourg: Publications Office of the European Union. pp. 17–40. https://data.europa.eu/doi/10.2777/58454

Dickson, A.G., Goyet, C., 1994. Handbook of methods for the analysis of the various parameters of the carbon dioxide system in seawater. Version 2. Oak Ridge National Lab., TN (United States). https://doi.org/10.2172/10107773

Dickson, A.G., Sabine, C.L., Christian, J.R., 2007. Guide to Best Practices for Ocean CO_2 measurements. Technical Report. PICES Special Publication 3. pp. 191. (ISBN 1-897176-07-4)

Dişa, D., Münnich, M., Vogt, M., Gruber, N., 2022. A space-time mosaic of seawater carbonate chemistry conditions in the north-shore Moorea coral reef system. Front. Mar. Sci. 9, 1004107. https://doi.org/10.3389/fmars.2022.1004107

Eyre, B.D., Cyronak, T., Drupp, P., Carlo, E.H.D., Sachs, J.P., Andersson, A.J., 2018. Coral reefs will transition to net dissolving before end of century. Science 359, 908–911. https://doi.org/10.1126/science.aao1118

Falter, J.L., Atkinson, M.J., Schar, D.W., Lowe, R.J., Monismith, S.G., 2011. Short-term coherency between gross primary production and community respiration in an algal-dominated reef flat. Coral Reefs 30, 53–58. https://doi.org/10.1007/s00338-010-0671-9

Falter, J.L., Lowe, R.J., Atkinson, M.J., Monismith, S.G., Schar, D.W., 2008. Continuous measurements of net production over a shallow reef community using a modified Eulerian approach. J. Geophys. Res. 113, C07035. https://doi.org/10.1029/2007JC004663

Falter, J.L., Lowe, R.J., Zhang, Z., McCulloch, M., 2013. Physical and Biological Controls on the Carbonate Chemistry of Coral Reef Waters: Effects of Metabolism, Wave Forcing, Sea Level, and Geomorphology. PLoS ONE 8, e53303. https://doi.org/10.1371/journal.pone.0053303

Frankignoulle, M., Gattuso, J.-P., Biondo, R., Bourge, I., Copin-Montégut, G., Pichon, M., 1996. Carbon fluxes in coral reefs. II. Eulerian study of inorganic carbon dynamics and measurements of air-sea CO_2 exchanges. Marine Ecology Progress Series 145, 123–132.

Gattuso, J.-P., Allemand, D., Frankignoulle, M., 1999a. Photosynthesis and Calcification at Cellular, Organismal and Community Levels in Coral Reefs: A Review on Interactions and Control by Carbonate Chemistry. Am Zool 39, 160–183. https://doi.org/10.1093/icb/39.1.160

Gattuso, J.-P., Frankignoulle, M., Smith, S.V., 1999b. Measurement of community metabolism and significance in the coral reef $\mathrm{CO_2}$ source-sink debate. Proceedings of the National Academy of Sciences 96, 13017–13022. https://doi.org/10.1073/pnas.96.23.13017

Gattuso, J.-P., Payri, C.E., Pichon, M., Delesalle, B., Frankignoulle, M., 1997. Primary production, calcification, and air-sea $\mathrm{CO_2}$ fluxes of a macroalgal-dominated coral reef community (Moorea, French Polynesia). J Phycol 33, 729–738. https://doi.org/10.1111/j.0022-3646.1997.00729.x

Gattuso, J.-P., Pichon, M., Delesalle, B., Canon, C., Frankignoulle, M., 1996. Carbon fluxes in coral reefs. I. Lagrangian measurement of community metabolism and resulting air-sea $\mathrm{CO_2}$ disequilibrium. Mar. Ecol. Prog. Ser. 145, 109–121. https://doi.org/10.3354/meps145109

Gray, S.E.C., DeGrandpre, M.D., Langdon, C., Corredor, J.E., 2012. Short-term and seasonal pH, $p\mathrm{CO_2}$ and saturation state variability in a coral-reef ecosystem. Global Biogeochem. Cycles 26, GB3012. https://doi.org/10.1029/2011GB004114

Gruber, R.K., Lowe, R.J., Falter, J.L., 2017. Metabolism of a tide-dominated reef platform subject to extreme diel temperature and oxygen variations. Limnol. Oceanogr. 62, 1701–1717. https://doi.org/10.1002/lno.10527

Guadayol, Ò., Silbiger, N.J., Donahue, M.J., Thomas, F.I.M., 2014. Patterns in Temporal Variability of Temperature, Oxygen and pH along an Environmental Gradient in a Coral Reef. PLoS ONE 9, e85213. https://doi.org/10.1371/journal.pone.0085213

Guinotte, J.M., Fabry, V.J., 2008. Ocean Acidification and Its Potential Effects on Marine Ecosystems. Annals of the New York Academy of Sciences 1134, 320–342. https://doi.org/10.1196/annals.1439.013

Herdman, L.M.M., Hench, J.L., Fringer, O., Monismith, S.G., 2017. Behavior of a wave-driven buoyant surface jet on a coral reef. JGR Oceans 122, 4088–4109. https://doi.org/10.1002/2016JC011729

Hoegh-Guldberg, O., Mumby, P.J., Hooten, A.J., Steneck, R.S., Greenfield, P., Gomez, E., Harvell, C.D., Sale, P.F., Edwards, A.J., Caldeira, K., Knowlton, N., Eakin, C.M., Iglesias-Prieto, R., Muthiga, N., Bradbury, R.H., Dubi, A., Hatziolos, M.E., 2007. Coral Reefs Under Rapid Climate Change and Ocean Acidification. Science 318, 1737–1742. https://doi.org/10.1126/science.1152509

Hofmann, G.E., Smith, J.E., Johnson, K.S., Send, U., Levin, L.A., Micheli, F., Paytan, A., Price, N.N., Peterson, B., Takeshita, Y., Matson, P.G., Crook, E.D., Kroeker, K.J., Gambi, M.C., Rivest, E.B., Frieder, C.A., Yu, P.C., Martz, T.R., 2011. High-Frequency Dynamics of Ocean pH: A Multi-Ecosystem Comparison. PLoS ONE 6, e28983. https://doi.org/10.1371/journal.pone.0028983

IPCC, 2019: IPCC Special Report on the Ocean and Cryosphere in a Changing Climate [Pörtner, H.-O., Roberts, D.C., Masson-Delmotte, V., Zhai, P., Tignor, M., Poloczanska, E., Mintenbeck, K., Alegría, A., Nicolai, M., Okem, A., Petzold, J., Rama, B., Weyer, N.M. (Eds).] Cambridge University Press, Cambridge, UK and New York, NY, USA. https://doi.org/10.1017/9781009157964

Kekuewa, S.A.H., Courtney, T.A., Cyronak, T., Kindeberg, T., Eyre, B.D., Stoltenberg, L., Andersson, A.J., 2021. Temporal and Spatial Variabilities of Chemical and Physical Parameters on the Heron Island Coral Reef Platform. Aquat Geochem 27, 241–268. https://doi.org/10.1007/s10498-021-09400-7

Kinsey, D.W., 1985. Metabolism, calcification and carbon production. Proceedings of the 5th international coral reef congress, Tahiti 4, 505–526.

Koweek, D., Dunbar, R.B., Rogers, J.S., Williams, G.J., Price, N., Mucciarone, D., Teneva, L., 2015a. Environmental and ecological controls of coral community metabolism on Palmyra Atoll. Coral Reefs 34, 339–351. https://doi.org/10.1007/s00338-014-1217-3

Koweek, D.A., Dunbar, R.B., Monismith, S.G., Mucciarone, D.A., Woodson, C.B., Samuel, L., 2015b. High-resolution physical and biogeochemical variability from a shallow back reef on Ofu, American

Samoa: an end-member perspective. Coral Reefs 34, 979–991. https://doi.org/10.1007/s00338-015-1308-9

Lantz, C.A., Atkinson, M.J., Winn, C.W., Kahng, S.E., 2014. Dissolved inorganic carbon and total alkalinity of a Hawaiian fringing reef: chemical techniques for monitoring the effects of ocean acidification on coral reefs. Coral Reefs 33, 105–115. https://doi.org/10.1007/s00338-013-1082-5

Lee, K., Tong, L.T., Millero, F.J., Sabine, C.L., Dickson, A.G., Goyet, C., Park, G.-H., Wanninkhof, R., Feely, R.A., Key, R.M., 2006. Global relationships of total alkalinity with salinity and temperature in surface waters of the world’s oceans. Geophys. Res. Lett. 33, L19605. https://doi.org/10.1029/2006GL027207

Levy, O., Dubinsky, Z., Schneider, K., Achituv, Y., Zakai, D., Gorbunov, M., 2004. Diurnal hysteresis in coral photosynthesis. Mar. Ecol. Prog. Ser. 268, 105–117. https://doi.org/10.3354/meps268105

Lowe, R.J., Falter, J.L., 2015. Oceanic Forcing of Coral Reefs. Annu. Rev. Mar. Sci. 7, 43–66. https://doi.org/10.1146/annurev-marine-010814-015834

Lowe, R.J., Falter, J.L., Monismith, S.G., Atkinson, M.J., 2009. Wave-Driven Circulation of a Coastal Reef–Lagoon System. Journal of Physical Oceanography 39, 873–893. https://doi.org/10.1175/2008JPO3958.1

Lueker, T.J., Dickson, A.G., Keeling, C.D., 2000. Ocean $p\mathrm{CO}_2$ calculated from dissolved inorganic carbon, alkalinity, and equations for K_1 and K_2: validation based on laboratory measurements of CO_2 in gas and seawater at equilibrium. Marine Chemistry 70, 105–119. https://doi.org/10.1016/S0304-4203(00)00022-0

McMahon, A., Santos, I.R., Schulz, K.G., Cyronak, T., Maher, D.T., 2018. Determining coral reef calcification and primary production using automated alkalinity, pH and $p\mathrm{CO}_2$ measurements at high temporal resolution. Estuarine, Coastal and Shelf Science 209, 80–88. https://doi.org/10.1016/j.ecss.2018.04.041

Meléndez, M., Salisbury, J., Gledhill, D., Langdon, C., Morell, J.M., Manzello, D., Rodriguez-Abudo, S., Musielewicz, S., Sutton, A., 2020. Seasonal Variations of Carbonate Chemistry at Two Western Atlantic Coral Reefs. JGR Oceans 125, e2020JC016108. https://doi.org/10.1029/2020JC016108

Mollica, N.R., Guo, W., Cohen, A.L., Huang, K.-F., Foster, G.L., Donald, H.K., Solow, A.R., 2018. Ocean acidification affects coral growth by reducing skeletal density. Proc Natl Acad Sci USA 115, 1754–1759. https://doi.org/10.1073/pnas.1712806115

Muehllehner, N., Langdon, C., Venti, A., Kadko, D., 2016. Dynamics of carbonate chemistry, production, and calcification of the Florida Reef Tract (2009–2010): Evidence for seasonal dissolution. Global Biogeochem. Cycles 30, 661–688. https://doi.org/10.1002/2015GB005327

Ohde, S., van Woesik, R., 1999. Carbon dioxide flux and metabolic processes of a coral reef, Okinawa. Bulletin of Marine Sciences 65, 559–576.

Orr, J.C., Epitalon, J.-M., Dickson, A.G., Gattuso, J.-P., 2018. Routine uncertainty propagation for the marine carbon dioxide system. Marine Chemistry 207, 84–107. https://doi.org/10.1016/j.marchem.2018.10.006

Orr, J.C., Fabry, V.J., Aumont, O., Bopp, L., Doney, S.C., Feely, R.A., Gnanadesikan, A., Gruber, N., Ishida, A., Joos, F., Key, R.M., Lindsay, K., Maier-Reimer, E., Matear, R., Monfray, P., Mouchet, A., Najjar, R.G., Plattner, G.-K., Rodgers, K.B., Sabine, C.L., Sarmiento, J.L., Schlitzer, R., Slater, R.D., Totterdell, I.J., Weirig, M.-F., Yamanaka, Y., Yool, A., 2005. Anthropogenic ocean acidification over the twenty-first century and its impact on calcifying organisms. Nature 437, 681–686. https://doi.org/10.1038/nature04095

Page, H.N., Courtney, T.A., De Carlo, E.H., Howins, N.M., Koester, I., Andersson, A.J., 2019. Spatiotemporal variability in seawater carbon chemistry for a coral reef flat in Kāneʻohe Bay, Hawaiʻi. Limnol Oceanogr 64, 913–934. https://doi.org/10.1002/lno.11084

Pezner, A.K., Courtney, T.A., Page, H.N., Giddings, S.N., Beatty, C.M., DeGrandpre, M.D., Andersson, A.J., 2021. Lateral, Vertical, and Temporal Variability of Seawater Carbonate Chemistry at Hog Reef, Bermuda. Front. Mar. Sci. 8, 562267. https://doi.org/10.3389/fmars.2021.562267

R Core Team, 2020. R: A language and environment for statistical computing. R Foundation for Statistical Computing, Vienna, Austria. https://www.R-project.org/

Rintoul, M.S., Courtney, T.A., Dohner, J.L., Giddings, S.N., Kekuewa, S.A.H., Mitarai, S., Monismith, S.G., Pezner, A.K., Andersson, A.J., 2022. The Effects of Light Intensity and Flow Speed on Biogeochemical Variability within a Fringing Coral Reef in Onna-son, Okinawa, Japan. JGR Oceans 127, e2021JC018369. https://doi.org/10.1029/2021JC018369

Roberts, H.H., Suhayda, J.N., 1983. Wave-current interactions on a shallow reef (Nicaragua, Central America). Coral Reefs 1, 209–214.

Schneider, K., Levy, O., Dubinsky, Z., Erez, J., 2009. In situ diel cycles of photosynthesis and calcification in hermatypic corals. Limnol. Oceanogr. 54, 1995–2002. https://doi.org/10.4319/lo.2009.54.6.1995

Schönberg, C.H.L., Fang, J.K.H., Carreiro-Silva, M., Tribollet, A., Wisshak, M., 2017. Bioerosion: the other ocean acidification problem. ICES Journal of Marine Science 74, 895–925. https://doi.org/10.1093/icesjms/fsw254

Shamberger, K.E.F., Feely, R.A., Sabine, C.L., Atkinson, M.J., DeCarlo, E.H., Mackenzie, F.T., Drupp, P.S., Butter, D.A., 2011. Calcification and organic production on a Hawaiian coral reef. Marine Chemistry 127, 64–75. https://doi.org/10.1016/j.marchem.2011.08.003

Sharma, S., Swayne, D.A., Obimbo, C., 2015. Automating the Smoothing of Time Series Data. J Environ Anal Toxicol 05, 1000304. https://doi.org/10.4172/2161-0525.1000304

Shaw, E.C., McNeil, B.I., Tilbrook, B., 2012. Impacts of ocean acidification in naturally variable coral reef flat ecosystems. J. Geophys. Res. 117, C03038. https://doi.org/10.1029/2011JC007655

Shaw, E.C., Phinn, S.R., Tilbrook, B., Steven, A., 2015. Natural in situ relationships suggest coral reef calcium carbonate production will decline with ocean acidification. Limnology & Oceanography 60, 777–788. https://doi.org/10.1002/lno.10048

Silverman, J., Lazar, B., Cao, L., Caldeira, K., Erez, J., 2009. Coral reefs may start dissolving when atmospheric CO_2 doubles. Geophys. Res. Lett. 36, L05606. https://doi.org/10.1029/2008GL036282

Soulsby, R., 1997. Dynamics of Marine Sands: A manual for practical applications, Thomas Telford Publications. ed.

Suzuki, A., Kawahata, H., 2003. Carbon budget of coral reef systems: an overview of observations in fringing reefs, barrier reefs and atolls in the Indo-Pacific regions. Tellus B: Chemical and Physical Meteorology 55, 428–444. https://doi.org/10.3402/tellusb.v55i2.16761

Taebi, S., Lowe, R.J., Pattiaratchi, C.B., Ivey, G.N., Symonds, G., Brinkman, R., 2011. Nearshore circulation in a tropical fringing reef system. J. Geophys. Res. 116, C02016. https://doi.org/10.1029/2010JC006439

Takeshita, Y., Cyronak, T., Martz, T.R., Kindeberg, T., Andersson, A.J., 2018. Coral Reef Carbonate Chemistry Variability at Different Functional Scales. Front. Mar. Sci. 5, 175. https://doi.org/10.3389/fmars.2018.00175

Tedetti, M., Bigot, L., Turquet, J., Guigue, C., Ferretto, N., Goutx, M., Cuet, P., 2020. Influence of Freshwater Discharges on Biogeochemistry and Benthic Communities of a Coral Reef Ecosystem (La Réunion Island, Indian Ocean). Front. Mar. Sci. 7, 596165. https://doi.org/10.3389/fmars.2020.596165

Teneva, L., Dunbar, R.B., Mucciarone, D.A., Dunckley, J.F., Koseff, J.R., 2013. High-resolution carbon budgets on a Palau back-reef modulated by interactions between hydrodynamics and reef metabolism. Limnol. Oceanogr. 58, 1851–1870. https://doi.org/10.4319/lo.2013.58.5.1851

Thomson, R.E., Emery, W.J., 2014. Data Analysis Methods in Physical Oceanography, 3rd ed. Elsevier.

Tribollet, A., Chauvin, A., Cuet, P., 2019. Carbonate dissolution by reef microbial borers: a biogeological process producing alkalinity under different $p\mathrm{CO}_2$ conditions. Facies 65. https://doi.org/10.1007/s10347-018-0548-x

Tribollet, A., Godinot, C., Atkinson, M., Langdon, C., 2009. Effects of elevated $p\mathrm{CO}_2$ on dissolution of coral carbonates by microbial euendoliths. Global Biogeochem. Cycles 23, GB3008. https://doi.org/10.1029/2008GB003286

van Heuven, S., Pierrot, D., Rae, J.W.B., Lewis, E., Wallace, D.W.R., 2011. MATLAB program developed for CO_2 system calculations. ORNL/CDIAC-105b. Carbon Dioxide Information Analysis Center, Oak Ridge National Laboratory, U.S Department of Energy, Oak Ridge, Tennessee. https://doi.org/10.3334/CDIAC/otg.CO2SYS_MATLAB_v1.1

Warton, D.I., Duursma, R.A., Falster, D.S., Taskinen, S., 2012. smatr 3 - an R package for estimation and inference about allometrics lines. Methods in Ecology and Evolution 3, 257-259. https://doi.org/10.1111/j.2041-210X.2011.00153.x

Watanabe, A., Kayanne, H., Hata, H., Kudo, S., Nozaki, K., Kato, K., Negishi, A., Ikeda, Y., Yamano, H., 2006. Analysis of the seawater CO_2 system in the barrier reef-lagoon system of Palau using total alkalinity-dissolved inorganic carbon diagrams. Limnol. Oceanogr. 51, 1614–1628. https://doi.org/10.4319/lo.2006.51.4.1614

Winter, G., Castelle, B., Lowe, R.J., Hansen, J.E., McCall, R., 2020. When is flow re-entrainment important for the flushing time in coastal reef systems? Continental Shelf Research 206, 104194. https://doi.org/10.1016/j.csr.2020.104194

Yamano, H., Kayanne, H., Yonekura, N., Nakamura, H., Kudo, K., 1998. Water circulation in a fringing reef located in a monsoon area: Kabira Reef, Ishigaki Island, Southwest Japan. Coral Reefs 17, 89–99. https://doi.org/10.1007/s003380050101

Yates, K.K., Halley, R.B., 2006. CO_3^{2-} concentration and pCO_2 thresholds for calcification and dissolution on the Molokai reef flat, Hawaii. Biogeosciences 3, 357–369. https://doi.org/10.5194/bg-3-357-2006

Zhang, Z., Falter, J., Lowe, R., Ivey, G., 2012. The combined influence of hydrodynamic forcing and calcification on the spatial distribution of alkalinity in a coral reef system. J. Geophys. Res. 117, C04034. https://doi.org/10.1029/2011JC007603

Zhang, Z., Lowe, R., Falter, J., Ivey, G., 2011. A numerical model of wave- and current-driven nutrient uptake by coral reef communities. Ecological Modelling 222, 1456–1470. https://doi.org/10.1016/j.ecolmodel.2011.01.014

Figures captions

Fig. 1. Map of the study area showing the location of the sampling stations on the reef flat of La Saline fringing reef (blue) and offshore (red) at La Reunion Island.

Fig. 2. Offshore water depth (m, black line) and current speeds *u* (m.s^{-1}) recorded in 2019 projected on a) the cross-shore axis and b) the alongshore axis.

Fig. 3. Hydrodynamics records, mean diel curves (for Trou d'Eau in April 2021) and individually time series of each day of PAR (µmol.m^{-2}.s^{-1}), temperature T (°C), dissolved oxygen concentration (DO, mmolO$_2$.m^{-3}) and pH$_T$ on the reef flat (dashed lines) and offshore (solid blue lines). At the top, the graphs illustrate the principal components analysis of the currents illustrated by ellipses (showing the major and minor semi-axis of current variability), the direction and intensity of the mean current illustrated by arrows and all measurements are shown as gray ticks. For the mean diel curves, standard deviations around averages are given in transparency. For dashed lines, each type of line represents one measurement day (including half-days).

Fig. 4. Records of: a. water depth (m), b. depth-averaged current speeds *U* (m.s^{-1}) and directions, c. PAR (µmol.m^{-2}.s^{-1}), d. temperature T (°C), e. dissolved oxygen concentration (DO, mmol.m^{-3}) and pH$_T$ over 15 days on the Trou d'Eau reef flat in April 2021. For the current record, the length of the sticks is proportional to the current speed and the direction of the sticks indicates the direction of the current. Gray lines correspond to raw data and black lines correspond to the 6-hour smoothed data (LOWESS).

Fig. 5. Total alkalinity (TA, µmol.kg^{-1}) and dissolved inorganic carbon concentration (DIC, µmol.kg^{-1}) as a function of the sampling hour, all sampling sites and periods taken together. Black points are offshore samples and shaded area is the standard deviation around the mean of all offshore samples.

Fig. 6. TA as a function of DIC concentration, all sampling sites and periods taken together. The red contour point is the mean of all offshore values (± SD). Black contour points are reef flat samples. Points are colored according to the saturation state of aragonite ($\Omega_{aragonite}$). Vectors illustrate the direction of the effects of photosynthesis, respiration, calcification and dissolution of $CaCO_3$ on TA and DIC. In reef environments, the impacts of photosynthesis and respiration on TA are usually negligible due to a higher stoichiometry (C:N:P ratio) than in marine plankton (Gattuso et al., 1999b).

Tables

Table 1

Mean (± SD) of offshore temperature (T), salinity (S), dissolved oxygen concentration (DO), pH_T, pH_T at 25°C, total alkalinity (TA), dissolved inorganic carbon concentration (DIC), saturation state of aragonite ($\Omega_{aragonite}$), partial pressure of CO_2 (pCO_2) and partial pressure of CO_2 at 25°C for warm and cold seasons. Values are significantly different between seasons (*p*-value < 0.0001), except for salinity (*p*-value = 0.35). Values in bold are measured parameters.

	T (°C)	S	DO (mmol.m^{-3})	pH_T	pH_T at 25°C	TA (µmol.kg^{-1})	DIC (µmol.kg^{-1})	$\Omega_{aragonite}$	pCO_2 (µatm)	pCO_2 at 25°C (µatm)
Warm Season	**27.6 (± 0.2)**	**34.99 (± 0.10)**	**202 (± 5)**	**8.02 (± 0.01)**	8.06 (± 0.01)	**2289 (± 4)**	1978 (± 5)	3.55 (± 0.06)	412 (± 13)	374 (± 10)
Cold Season	**24.3 (± 0.4)**	**35.00 (± 0.01)**	**219 (± 4)**	**8.05 (± 0.01)**	8.04 (± 0.01)	**2297 (± 4)**	1998 (± 6)	3.36 (± 0.04)	388 (± 7)	398 (± 8)

Table 2
Key physical parameters recorded on the reef flat of La Saline fringing reef: temperature (°C), salinity and PAR (µmol.m^{-2}.s^{-1}). TDE: Trou d'Eau; LIV: Livingstone; TOB: Toboggan

	T (°C)		**S**		**PAR (µmol.m^{-2}.s^{-1})**
	Mean (± SD)	Range	Mean (± SD)	Range	Range
TDE - Apr 2021 (N=1437)	27.3 (± 0.6)	26.1-29.3	34.95 (± 0.07)	34.78-35.12	0-1160
LIV - Oct 2021 (N=466)	24.3 (± 0.8)	22.9-26.6	35.01 (± 0.04)	34.95-35.08	0-1260
TOB - Oct 2021 (N=265)	24.7 (± 0.3)	24.3-26.1	35.01 (± 0.02)	34.96-35.04	0-1276
TDE - Oct 2021 (N=197)	25.2 (± 0.5)	24.6-26.4	35.02 (± 0.02)	34.94-35.04	0-1302
TOB - Jun 2022 (N=305)	25.1 (± 0.5)	24.0-26.1	35.07 (± 0.03)	35.01-35.16	0-977

Table 3

Key biogeochemical parameters recorded on the reef flat of La Saline fringing reef: dissolved oxygen (DO) concentration (mmol.m^{-3}) and pH$_T$ values. The mean diel range is estimated from mean diel curves (max - min of mean diel curves). TDE: Trou d'Eau; LIV: Livingstone; TOB: Toboggan.

	DO (mmol.m^{-3})				**pH$_T$**			
	Mean (± SD)	Min	Max	Mean diel range	Mean (± SD)	Min	Max	Mean diel range
TDE - Apr 2021 (N=1437)	207 (± 47)	130	350	107	7.99 (± 0.08)	7.80	8.18	0.20
LIV - Oct 2021 (N=466)	218 (± 52)	140	339	121	8.02 (± 0.09)	7.86	8.21	0.23
TOB - Oct 2021 (N=265)	213 (± 30)	163	297	88	8.00 (± 0.06)	7.88	8.14	0.19
TDE - Oct 2021 (N=197)	227 (± 50)	166	340	118	8.02 (± 0.08)	7.89	8.19	0.18
TOB - Jun 2022 (N=305)	201 (± 37)	148	302	91	8.00 (± 0.07)	7.88	8.15	0.17

Table 4

Key hydrodynamic parameters recorded on the reef flat of La Saline fringing reef: depth (m), direction of the mean flow θ (°), depth-averaged current speed projected on the direction of the mean flow u_x (m.s^{-1}) and on the normal of the direction of the mean flow u_y (m.s^{-1}). Angles are measured positively East and negatively West from geographic North. For u_x, positive values are directed on the mean current direction θ and for u_y, positive values are directed on θ + 270 °. TDE: Trou d'Eau; LIV: Livingstone; TOB: Toboggan.

	Depth (m)		**θ (°)**	**u_x (m.s^{-1})**		**u_y (m.s^{-1})**	
	Mean (± SD)	Range	Mean (± SD)	Mean (± SD)	Range	Mean (± SD)	Range
TDE - Apr 2021 (N=4320)	1.23 (± 0.15)	0.89-1.70	34 (± 48)	0.046 (± 0.044)	-0.16-0.29	-2.45.10^{-4} (± 0.032)	-0.21-0.17
LIV - Oct 2021 (N=1425)	1.10 (± 0.13)	0.86-1.39	-17 (± 43)	0.024 (± 0.033)	-0.12-0.18	1.97.10^{-4} (± 0.028)	-0.11-0.11
TOB - Oct 2021 (N=816)	1.01 (± 0.16)	0.77-1.40	63 (± 40)	0.048 (± 0.042)	-0.08-0.22	1.69.10^{-5} (± 0.041)	-0.21-0.17
TDE - Oct 2021 (N=603)	1.20 (± 0.13)	0.92-1.49	36 (± 46)	0.046 (± 0.048)	-0.13-0.25	-1.55.10^{-4} (± 0.026)	-0.08-0.08
TOB - Jun 2022 (N=863)	0.95 (± 0.16)	0.61-1.24	9 (± 55)	0.069 (± 0.030)	-0.03-0.18	-2.93.10^{-4} (± 0.029)	-0.09-0.11

Highlights:

- Seawater chemistry on La Saline reef is modulated by hydrodynamics and geomorphology
- Dissolved oxygen and pH_T variations are decoupled in time on La Saline fringing reef
- Water exiting the reef by the channels is re-entrained on the reef flat
- Water re-entrained on the reef flat appears TA depleted
- The Eulerian approach can lead to errors in the estimation of $CaCO_3$ budgets

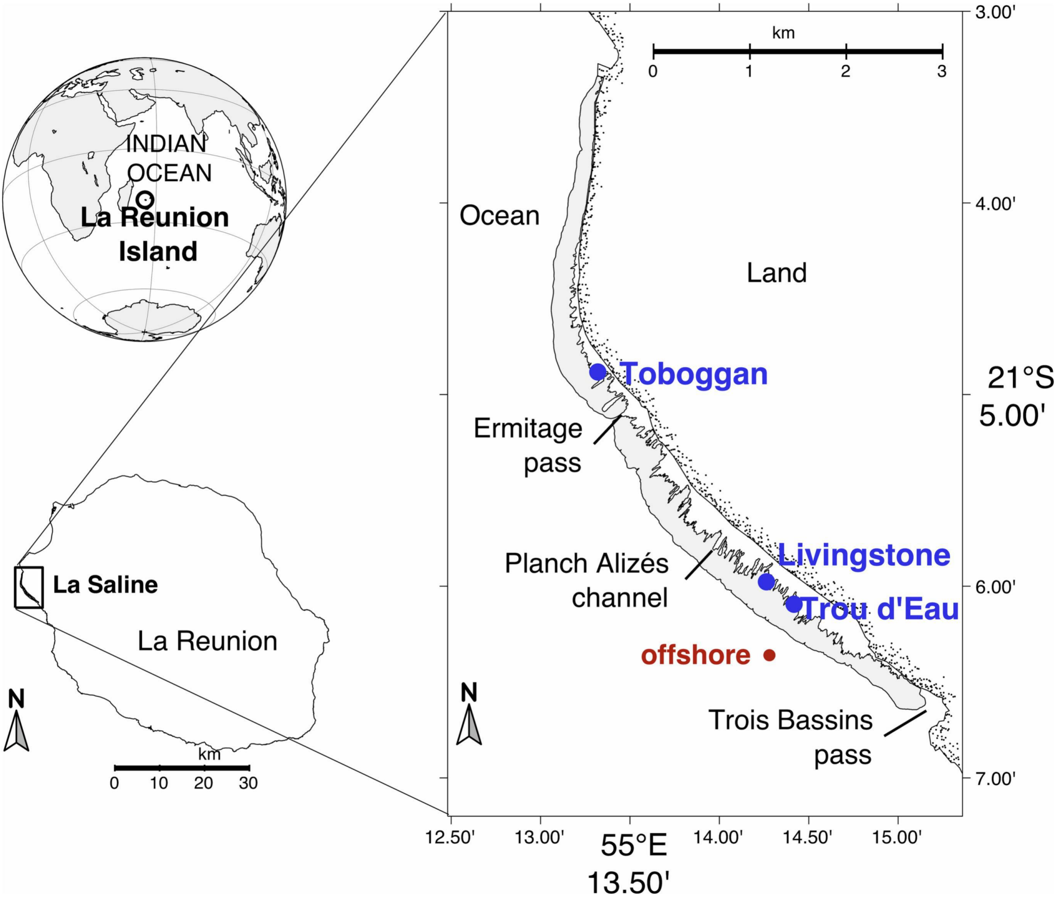
INDIAN
OCEAN
La Reunion
Island
La Saline
La Reunion
N
km
0
10
20
30
3.00'
4.00'
21°S
5.00'
6.00'
7.00'
km
0
1
2
3
Ocean
Land
Toboggan
Ermitage
pass
Planch Alizés
channel
Livingstone
Trou d'Eau
offshore
Trois Bassins
pass
N
12.50'
13.00'
55°E
13.50'
14.00'
14.50'
15.00'

Figure 1

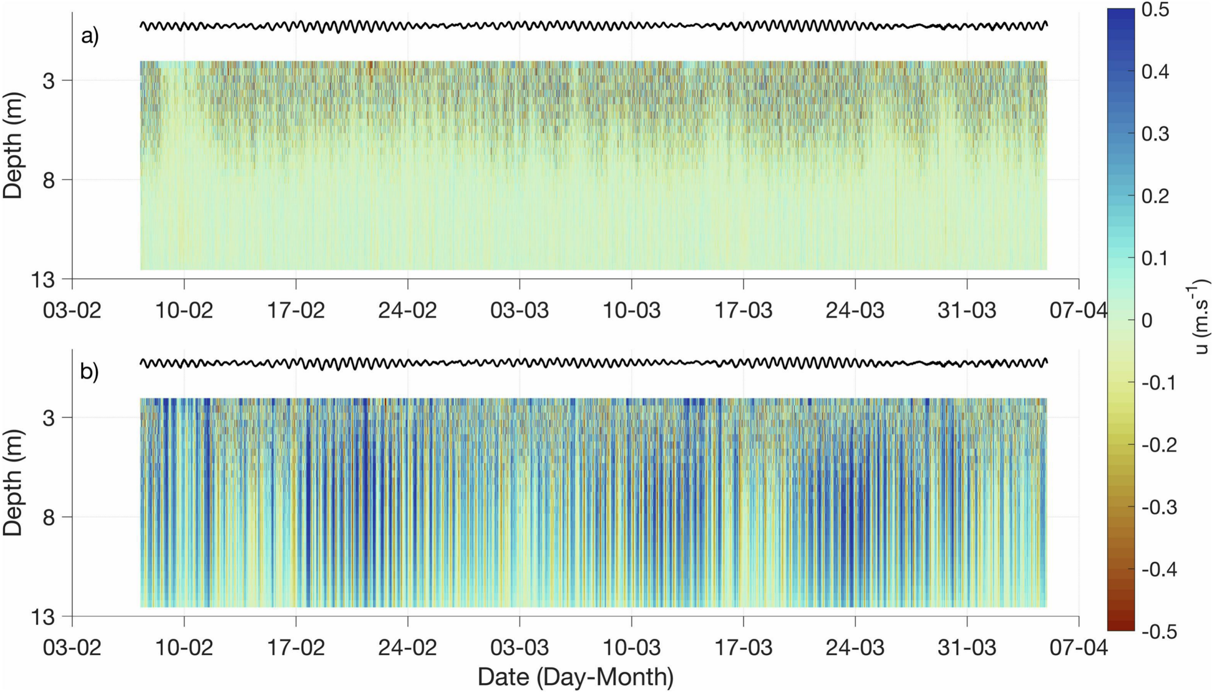

a)
b)
Depth (m)
3
8
13
03-02
10-02
17-02
24-02
03-03
10-03
17-03
24-03
31-03
07-04
Date (Day-Month)
u (m.s^{-1})
0.5
0.4
0.3
0.2
0.1
0
-0.1
-0.2
-0.3
-0.4
-0.5

Figure 2

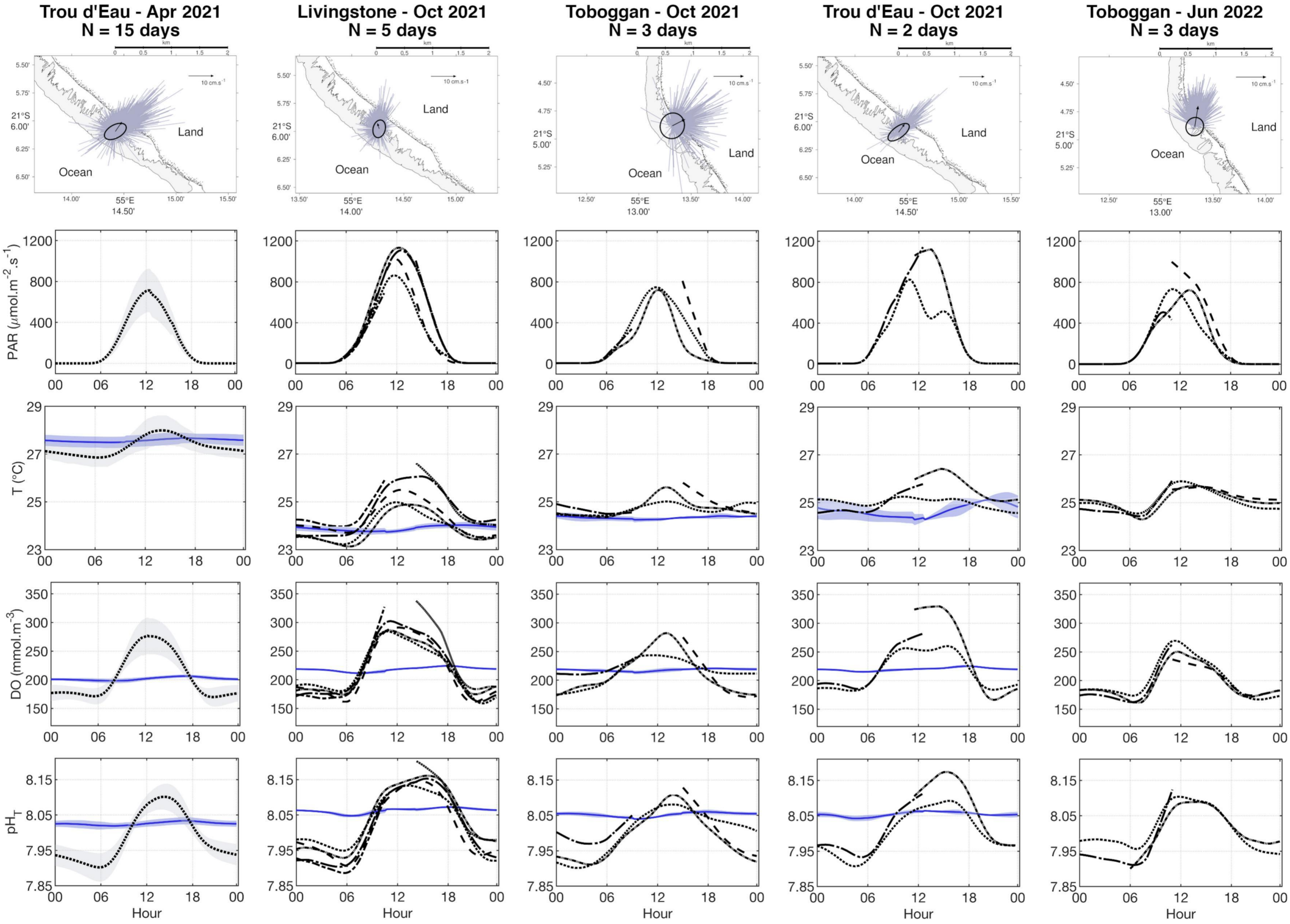
Trou d'Eau - Apr 2021
N = 15 days
Livingstone - Oct 2021
N = 5 days
Toboggan - Oct 2021
N = 3 days
Trou d'Eau - Oct 2021
N = 2 days
Toboggan - Jun 2022
N = 3 days
km
0 0.5 1 1.5 2
10 cm.s-1
Land
Ocean
21°S
55°E
PAR (μmol.m-2.s-1)
T (°C)
DO (mmol.m-3)
pHT
Hour
00 06 12 18 00

Figure 3

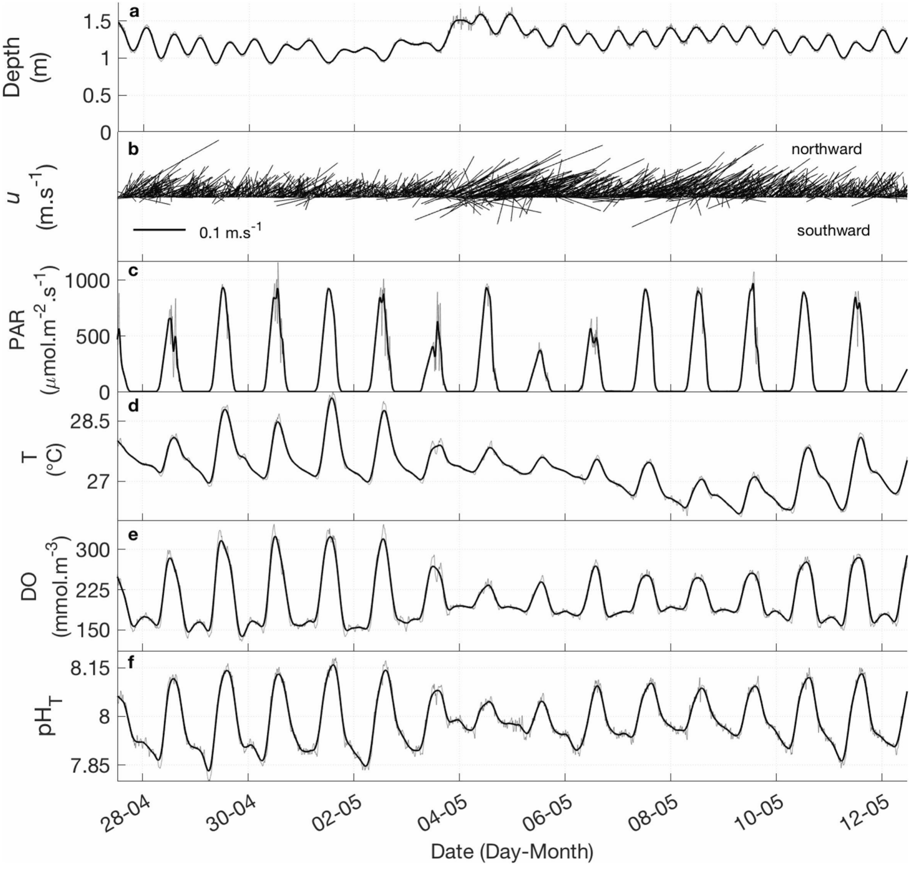
a
Depth (m)
0
0.5
1
1.5
b
u (m.s^{-1})
northward
southward
0.1 m.s^{-1}
c
PAR (μmol.m^{-2}.s^{-1})
0
500
1000
d
T (°C)
27
28.5
e
DO (mmol.m^{-3})
150
225
300
f
pH$_T$
7.85
8
8.15
28-04
30-04
02-05
04-05
06-05
08-05
10-05
12-05
Date (Day-Month)

Figure 4

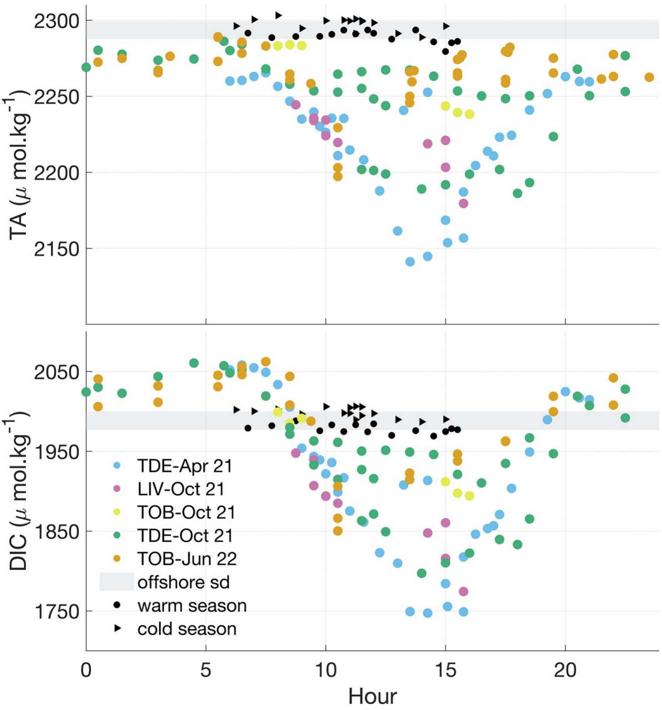

2300
2250
2200
2150
TA (μ mol.kg^{-1})
2050
1950
1850
1750
DIC (μ mol.kg^{-1})
TDE-Apr 21
LIV-Oct 21
TOB-Oct 21
TDE-Oct 21
TOB-Jun 22
offshore sd
warm season
cold season
0
5
10
15
20
Hour

Figure 5

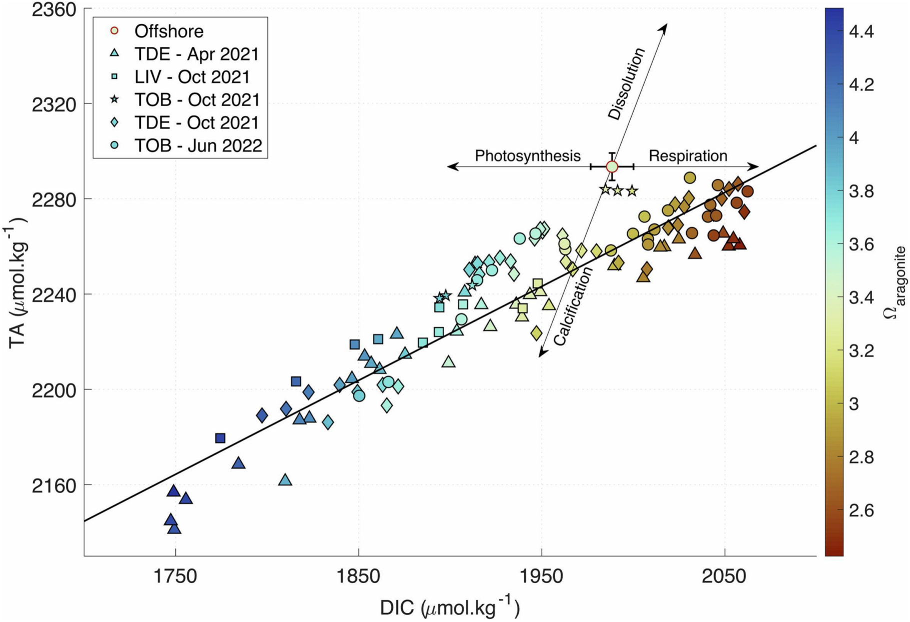
Offshore
TDE - Apr 2021
LIV - Oct 2021
TOB - Oct 2021
TDE - Oct 2021
TOB - Jun 2022
Dissolution
Photosynthesis
Respiration
Calcification
TA (µmol.kg⁻¹)
DIC (µmol.kg⁻¹)
2360
2320
2280
2240
2200
2160
1750
1850
1950
2050
Ω aragonite
4.4
4.2
4
3.8
3.6
3.4
3.2
3
2.8
2.6

Figure 6